Extracellular synthesis of silver nanoparticle using yeast extracts: antibacterial and seed priming applications

Dae-Young Kim[1] · Min Kim[2] · Jung-Suk Sung[2] · Janardhan Reddy Koduru[3] · Shivraj Hariram Nile[4] · Asad Syed[5] · Ali H. Bahkali[5] · Chandra Shekhar Seth[6] · Gajanan Sampatrao Ghodake[1]

Abstract

The evolution and rapid spread of multidrug-resistant (MDR) bacterial pathogens have become a major concern for human health and demand the development of alternative antimicrobial agents to combat this emergent threat. Conventional intracellular methods for producing metal nanoparticles (NPs) using whole-cell microorganisms have limitations, including binding of NPs to cellular components, potential product loss, and environmental contamination. In contrast, this study introduces a green, extracellular, and sustainable methodology for the bio-materialization of silver NPs (AgNPs) using renewable resource cell-free yeast extract. These extracts serve as a sustainable, biogenic route for both reducing the metal precursor and stabilizing the surface of AgNPs. This method offers several advantages such as cost-effectiveness, environment-friendliness, ease of synthesis, and scalability. HR-TEM imaging of the biosynthesized AgNPs revealed an isotropic growth route, resulting in an average size of about ~ 18 nm and shapes ranging from spherical to oval. Further characterization by FTIR and XPS results revealed various functional groups, including carboxyl, hydroxyl, and amide contribute to enhanced colloidal stability. AgNPs exhibited potent antibacterial activity against tested MDR strains, showing particularly high efficacy against Gram-negative bacteria. These findings suggest their potential role in developing alternative treatments to address the growing threat of antimicrobial resistance. Additionally, seed priming experiments demonstrated that pre-sowing treatment with AgNPs improves both the germination rate and survival of *Sorghum jowar* and *Zea mays* seedlings.

Key points
●*Yeast extract enables efficient, cost-effective, and eco-friendly AgNP synthesis.*
●*Biosynthesized AgNPs showed strong antibacterial activity against MDR bacteria.*
●*AgNPs boost seed germination and protect against seed-borne diseases.*

✉ Gajanan Sampatrao Ghodake
ghodakegs@gmail.com

1 Department of Biological and Environmental Science, Dongguk University-Seoul, Ilsandong-Gu, Goyang-Si 10326, Gyeonggi-Do, Republic of Korea

2 Department of Life Science, Dongguk University-Seoul, Biomedical Campus, 32 Dongguk-Ro, Ilsanadong-Gu, Goyang-Si 10326, Gyeonggi-Do, Republic of Korea

3 Department of Environmental Engineering, Kwangwoon University, Seoul 01897, Republic of Korea

4 Division of Food and Nutrition, DBT-National Agri-Food Biotechnology Institute, Mohali, Sahibzada Ajit Singh Nagar 140308, Punjab, India

5 Department of Botany and Microbiology, College of Science, King Saud University, P.O. Box 2455, 11451 Riyadh, Saudi Arabia

6 Department of Botany, University of Delhi, New Delhi, Delhi 110007, India

Introduction

From a historical perspective, antibiotics have served as powerful tools in the fight against bacterial and fungal pathogens (Torky et al. 2022). Although the rise of MDR pathogens is a global phenomenon affecting humans, animals, and the environment, it is particularly prevalent in response to conventional antibiotics (Sheikh et al. 2022). Regrettably, the widespread availability of antibiotics has led to their misuse and overuse, both in human healthcare and veterinary medicine (Adebisi 2023). The inappropriate use of antibiotics and their traces in environmental settings accelerates the evolutionary pressures of selecting antibiotic-resistant strains of bacteria, contributing to a growing public health crisis (Agreles et al. 2022). In antimicrobial resistance (AMR), bacterial pathogens evolve different mechanisms that effectively neutralize antibiotics, rendering standard treatments ineffective and leading to prolonged, potentially fatal infections. Thus, AMR has emerged as one of the most pressing public health crises, leading to increased mortality and morbidity on a global scale (Kumar et al. 2023b). Alarmingly, if current mitigation strategies fail, the death toll could rise to an estimated 10 million per year by 2050 (Ali et al. 2020). In addition, the development of new antibiotics has not kept pace with the emergence of superbugs, due to a combination of complex regulatory policies, lengthy clinical trials, and fluctuating demand (Altarac et al. 2021). Failure to address the growing threat of AMR could result in severe consequences, including excessive burden on healthcare systems, extended hospital stays, increased treatment costs, and threatened lives worldwide (Ayukekbong et al. 2017; Dadgostar 2019). To confront this challenge and secure a healthier future, there is an urgent need to accelerate the discovery of new antibiotics, preserve the effectiveness of existing ones, and innovate new classes of antibacterial agents.

To counter the growing threat of AMR, nanomaterials have rapidly emerged as potential antibacterial agents, with a surge in research and development activity (Hochvaldová et al. 2022). The field of antibacterial nanomaterials has seen a series of exciting advancements (Garg et al. 2022), as various nanomaterials have been validated for their potent antibacterial properties against MDR bacterial pathogens (Noorafsha et al. 2022). Nanoantibiotics, including metal nanoparticles (Zheng et al. 2022) and their nanocomposites (Chakraborty et al. 2022), exhibit inherent antibacterial capabilities, positioning them as promising alternatives to traditional antibiotics. Among these, silver nanoparticles (AgNPs) have found applications in a variety of commercial products (Potter et al. 2019), water purification (Ghodake et al. 2020b), medical device disinfection (Deshmukh et al. 2019), and the fight against MDR bacteria (Bano et al. 2023). The scope for AgNPs in developing antibacterial applications continues to expand in biomedical research (Pallavicini and Dacarro 2018), and prioritizing their safety becomes paramount, especially when tackling the MDR issue.

In nanosynthesis, principles of "green chemistry" have been established, aiming for bio-inspired designs that minimize negative impacts on human health and the environment (Shukla et al. 2008; Varjovi et al. 2023). By avoiding hazardous chemicals and solvents, safer synthesis protocols can be implemented, reducing the cytotoxicity of nanomedicines (Ali et al. 2020; Iravani et al. 2014). Therefore, it is essential to assess safer protocols for synthesizing AgNPs and pave the way for innovative and effective antibacterial strategies, addressing the urgent need to mitigate AMR. In addition, improving the physicochemical properties and enhancing the production of AgNPs through bio-materialization remain areas of active research (Arif and Uddin 2021; Lethongkam et al. 2023). Currently, the microbial synthesis of metal NPs, either through intracellular or extracellular methods, has gained significant attention in the scientific community (Ghosh et al. 2021). This involves a range of biosynthesis methods that utilize microorganisms—such as bacteria, fungi, yeast, and algae—as well as their extracts, which act as reducing and passivating agents (Vidyasagar et al. 2023).

In particular, intracellular synthesis using whole-cell microorganisms leads to the accumulation of metal ions within the cytoplasm. This is typically followed by the reduction of metal precursors, resulting in the formation of zero-valent NPs or the uptake of existing NPs (Augustine et al. 2020). This approach often leads to strong binding of NPs to cellular components (Arif and Uddin 2021), needing extensive downstream processing like ultrasonication or the use of detergents for purification (Bahrulolum et al. 2021). Such methods can potentially result in the loss of nanoproducts and environmental contamination (Hulkoti and Taranath 2014). Among the various biological methods, extracellular biosynthesis using cell-free extracts has received considerable attention, as it aligns more closely with green chemistry principles (Shukla et al. 2008). Furthermore, extracellular biosynthesis generally follows facile, cost-effective, energy-efficient, and safer protocols, facilitating ease of synthesis and purification with minimal downstream processing (Saravana Kumar et al. 2015).

This biosynthesis method relies on the reduction capabilities of biomolecules present in the cell-free yeast extracts, which collectively contribute to the effective conversion of Ag salts into AgNPs. By utilizing renewable and natural food-grade, cell-free yeast extracts, this method aligns with the principles of green chemistry. To obtain a safe and potent antibacterial agent, the impact of various synthesis parameters was evaluated systematically, including pH,

concentration of AgNO$_3$, and the amount of yeast extract, on the yield and optical properties of the AgNPs. The colloidal dispersions of AgNPs prepared using yeast extract remain stable due to multiple biomolecules that serve as excellent passivating agents, providing robust protection against undesirable aggregation. The biomolecules involved in capping the AgNPs possess nutritional content that is thought to potentially attract bacterial pathogens, thereby offering the possibility of addressing the challenges posed by AMR. Implementing AgNP-based seed priming provides a sustainable alternative to chemical treatments, reduces dependence on synthetic or hazardous agrochemicals, and supports environment-friendly seed treatment agents.

Materials and methods

Materials

Silver nitrate, Gram's iodine solution, poly-L-lysine, glutaraldehyde, and crystal violet reagent were procured from Sigma-Aldrich Chemicals. A standard solution of sodium hydroxide (NaOH, 1 M) and phosphate buffer was acquired from Bio-sensing Chemicals in Daejeon, Korea. Analytical-grade dried powder of nutrient broth, cell-free yeast extracts, and agar powder were obtained from Becton Dickinson Chemicals. MDR bacterial strains, including gram-positive *Staphylococcus aureus* [KCCM 11335] and gram-negative *Escherichia coli* [KCCM 11234], were purchased from the Korean Culture Center of Microorganisms (Seoul, Korea). Nanopure distilled water (DI) was sourced from a Thermo Scientific apparatus and was used for reagent preparation and AgNP biosynthesis.

Biosynthesis of AgNPs

Cell-free yeast extract (*Saccharomyces cerevisiae*) is a hydrolysate of the water-soluble fraction of biomolecules, which include partially degraded nucleic acids, proteins, and peptides (Tao et al. 2023). This mixture of nutrients is commonly used as a nitrogen source in microbial growth media because it contains nucleic acids, peptides, amino acids, carbohydrates, vitamins, and minerals (Tomé 2021). In this study, we propose using yeast extract—rich in diverse biomolecules with functional groups such as carboxyl, hydroxyl, amino, and thiol—to advance the biosynthesis of AgNPs (Heuer-Jungemann et al. 2019). A stock solution of yeast extract, with a concentration of about 0.4% (wt/v), was dissolved in DI water. This solution was gently mixed and used freshly in the AgNP synthesis experiments. The effects of various biosynthesis parameters were examined in a 10 mL reaction mixture at 65 °C for 24 h. This includes examining the influence of pH, yeast extract

concentration, and the metal precursor AgNO$_3$ to achieve desired optical and structural properties, enhance yield, and improve the stability of colloidal dispersions. The influence of alkaline pH was assessed by formulating reaction solutions with increasing NaOH concentration range from 0.5 to 6 mM while keeping the cell-free yeast extract concentration (0.05% wt/v) and AgNO$_3$ (0.5 mM) constant. To investigate the influence of cell-free yeast extract, we systematically increased its initial concentration in a range from 0.004 to 0.16% (w/v), while maintaining constant concentrations of NaOH (2 mM) and AgNO$_3$ (0.5 mM). Furthermore, the kinetics of AgNP production and the efficiency of the method were assessed using initial AgNO$_3$ concentration ranging from 0.5 mM to 3.0 mM, while keeping the concentrations of NaOH and yeast extract constant at 2 mM and 0.05% w/v, respectively. Finally, biosynthesis of AgNPs was conducted using the optimized reaction conditions (NaOH (2 mM), yeast extract (0.05% w/v), and AgNO$_3$ (0.5 mM)), adhering to the principles of green chemistry. The biosynthesized AgNPs under optimal conditions were systematically characterized and used to evaluate their antibacterial and seed-priming applications.

Characterization of AgNPs

UV–Vis absorbance spectroscopy of AgNP samples was examined using a UV–Vis spectrophotometer (Optizen 2120, Mecasys, South Korea). Samples with varying concentrations of AgNO$_3$ were carefully diluted with DI water at a ratio of about 0.2:0.8 (AgNPs to DI water) before measurements. Imaging of AgNPs and their selected area electron diffraction (SAED) pattern was performed using a high-resolution transmission electron microscope (HR-TEM) Technai G2 instrument (Ames Laboratory, Ames, Iowa). For HR-TEM analysis, 20 µL suspension of AgNPs was carefully drop-cast onto Formvar carbon-coated copper grids (Ted Pella Inc.) to prepare the samples. X-ray photoelectron spectroscopy (XPS) was carried out using a Thermo Fisher Scientific instrument to examine the oxidation state and surface chemistry of the AgNPs. Survey spectra and core-level XPS spectra for Ag (3d), O (1 s), and N (1 s) were recorded on the Theta Probe Angle-Resolved-XPS System. The C (1 s) line with a binding energy of 284.5 eV served as an internal reference for calibration purposes. Fourier-transform infrared spectroscopy (FTIR) of cell-free yeast extract powder and AgNP samples was recorded using attenuated total reflectance equipment from Thermo Fisher Scientific. X-ray diffraction (XRD) investigation was performed on thin films of AgNPs with a PANalytical X'Pert Pro diffractometer. These characterization techniques allowed for a comprehensive analysis of the AgNPs, including their size, morphology, crystal structure, chemical composition, and surface chemistry.

Bacterial cell culture

The antibacterial efficacy of AgNPs was assessed using MDR strains using various microbiology methods, including cell viability assays, colony-forming unit (CFU) counts, disk diffusion tests, and morphological imaging. To begin the experiments, bacterial strains were plated on nutrient agar and incubated at 37 °C for a period of 24 h. Subsequently, cells harvested from these cultures were introduced into a nutrient broth. The resulting bacterial cultures were allowed to grow in a shaking incubator at 120 rpm and 37 °C until reaching the early stationary growth phase. Cultures were then separated by centrifuging at a speed of 7000 rpm for 5 min. The resulting bacterial pellet was then carefully resuspended in a sterile phosphate buffer (50 mM, pH 7.2). This suspension was immediately used to prepare an inoculum with a cell concentration of about 2×10^5 CFU/mL.

Bacterial cell viability assay

Cell viability assays were conducted to examine the effects of AgNPs on the viability of the bacterial strains being tested. AgNPs were added to sterile LB broth for *S. aureus* and NB broth for *E. coli* at varying concentrations—from 1 to 20 ppm for a narrow concentration range, and 20 to 200 ppm for a broad concentration range. Fresh cultures of the bacterial pathogens under study were inoculated into their respective treatment samples. These treated bacterial cells were then incubated under shaking conditions at 120 rpm and 37 °C. Turbidity measurements were conducted three times at a 600-nm wavelength utilizing an ELISA reader from Tecan, Männedorf, Switzerland. Statistical analysis of the collected data was carried out via one-way ANOVA. The lowest concentration of AgNPs that inhibited bacterial growth was identified as the minimal inhibitory concentration (MIC). The turbidity assay allowed for the measurement of cell density and provided an estimate of bacterial growth and viability. The assay was performed using sterile cell-free yeast extracts under identical culture conditions to serve as a negative control. No turbidity in the treated samples indicated diminished bacterial cell viability, likely due to the inhibitory effects of AgNPs on bacterial growth.

Colony count assay

The antibacterial efficiency of the AgNPs was measured using the colony count method. Bacterial cultures in the early stationary phase were separately incubated with AgNPs at concentrations ranging from 30 to 100 ppm for 4 h at 37 °C. After the bacterial cultures underwent treatment, 150 μL samples were uniformly applied to nutrient agar surfaces and subjected to a 24-h incubation period at

a temperature of 37 °C in a static environment. To evaluate antibacterial effects, the visible bacterial CFUs on the nutrient agar plates were counted. The colony count provides an estimate of viable bacterial cells that were able to grow and form visible colonies on the agar surface. Bacterial cells seeded onto sterile nutrient agar plates without any antibacterial agents served as negative controls. The relative CFU reduction (%) was calculated using an equation previously reported by Shao et al. to quantify the decrease in CFU relative to the negative control group (Shao et al. 2015).

Relative CFU killing (%) = (1 − number of colonies on AgNP-treated plates/number of colonies on control plates) × 100.

Disc diffusion assay

The inhibitory effects of the biosynthesized AgNPs on bacterial growth were evaluated using the zone of inhibition method. Paper discs were prepared and loaded with 50 μL of aqueous AgNP dispersions at varying concentrations (10, 20, 30, 50, 100, and 200 ppm). These discs were then dried and sterilized under a UV lamp for 45 min. To begin the assay, nutrient agar plates were inoculated with test bacteria at a cell density of about 1×10^5 CFU per plate by evenly spreading the inoculum. AgNP-treated and sterilized discs were carefully inoculated, while sterile water-treated paper discs served as negative controls. The discs were placed carefully and ensured direct contact between the AgNPs and the bacterial culture. The nutrient agar plates, with the discs in place, were incubated under static conditions for 24 h at 37 °C. After this period, the inhibitory effects of the biosynthesized AgNPs on bacterial growth became evident as clear zones around the discs. These clear zones represent areas where bacterial growth was inhibited due to the antimicrobial properties of the AgNPs. The diameters of these zones of inhibition around each disc were recorded to evaluate the antimicrobial effectiveness of the AgNPs against bacterial pathogens.

Bacterial cells imaging

Optical microscopy and FE-SEM techniques were used to examine the morphological changes in bacterial cells following treatment with AgNPs. Bacterial cells in the early stationary growth phase were treated with AgNPs at below minimum inhibitory concentration of about 30 ppm and then subjected to gram staining according to established protocols (Ghodake et al. 2020a). Images of the AgNP-treated and gram-stained bacterial cells were captured using an optical microscope. This allowed for the assessment of any changes in cell morphology and shape induced by AgNP treatment. The gram staining procedure enabled optical visualization of morphological changes caused by the AgNPs. Bacterial cells

grown in a sterile culture medium without any antibacterial agents served as negative controls. Additionally, FE-SEM was employed to further investigate the morphological alterations in the tested bacteria. To prepare the samples, treated bacterial cells were fixed in a 2.5% glutaraldehyde solution and mounted on poly-L-lysine-coated coverslips. The fixed bacterial samples underwent a dehydration process using progressively higher concentrations of analytical-grade ethanol (ranging from 20 to 100%). Following drying, the specimens were coated with a thin layer of platinum and then subjected to imaging at multiple points using an FE-SEM from Hitachi S-4700, Tokyo, Japan. Both optical microscopy and FE-SEM were utilized to assess the morphological alterations in bacterial cells caused by AgNP treatment.

Seed priming studies

Two types of seeds, *Sorghum jowar* and *Zea mays*, were subjected to seed priming using various concentrations of AgNPs as the nano-priming agent. The priming process involved soaking the seeds in 10 mL of AgNP (10, 20, 30, 40, 50, 60, or 70 ppm) solution under dark conditions for 12 h at 24 °C. After priming, the treated seeds were carefully rinsed with DI water and dried at room temperature. To assess the effects of nano-priming on seed germination, germination assays were conducted in an incubator under alternating dark/light cycles of 12 h each at a temperature of 30 °C. Both control (unprimed) seeds and AgNP-primed seeds were included in the study. Petri dishes were prepared, each containing 20 seeds, and each variable was replicated at least four times. A seed with an emerged radicle measuring about 1.5 mm or more was considered fully germinated. The count of visibly germinated seeds was recorded over a 72-h period. To evaluate the impact of nano-priming, several germination parameters were examined, including the time taken for 50% germination, germination percentage, and mean germination time, as previously reported (Acharya et al. 2020). These parameters provided insights into the effects of AgNP-based nano-priming on the germination performance of the treated seeds. Overall, seed priming

with AgNPs offers a promising strategy for improving seed germination rates, seedling vigor, and management of seed-borne diseases in agriculture. This approach aligns with the goals of sustainable and environment-friendly practices, while also providing cost-effective solutions to farmers.

Results

Biosynthesis of AgNPs

This study, established a safer and more sustainable method for producing AgNPs, exploiting cell-free yeast extract as a benign and renewable resource to effectively reduce the silver precursor and stabilize the AgNPs. Initially, we attempted to synthesize AgNPs under alkaline and low-temperature conditions (25 to 45 °C). While these temperature conditions did yield AgNPs, the reaction rate was slow, and there was a propensity for producing mixed- or large-sized AgNPs. To address this challenge, we improved the reaction rate and tuned isotropic growth by elevating the temperature conditions to about 65 °C, while maintaining an alkaline environment. This strategic adjustment facilitated the classical nucleation and growth route, resulting in the more consistent and uniform formation of AgNPs. The effect of synthesis parameters—such as pH, cell-free yeast extract, and $AgNO_3$ concentration—were systematically evaluated under temperature conditions of about 65 °C. The optical properties and yield analysis of the resulting AgNPs were characterized by monitoring UV–vis spectrums.

When the synthesis process proceeded without NaOH, no evidence of AgNP formation was observed. UV–vis spectra of the AgNPs were examined by changes in the plasmon wavelength (λmax) and plasmon bandwidth ($\Delta\lambda$) as a function of NaOH concentration. Typically, characteristic surface plasmon resonance (SPR) peaks emerged around 420 nm, with minor redshift at elevated NaOH concentrations (Fig. 1a). This observation highlights the crucial role of an alkaline pH in enhancing the yield of AgNPs effectively. The slight shift in the UV–vis spectra toward a larger

Fig. 1 Effect of pH. **a** UV–Vis spectra of AgNPs at increasing concentration of NaOH and **b** absorbance intensity of AgNPs suspension at increasing concentration of NaOH
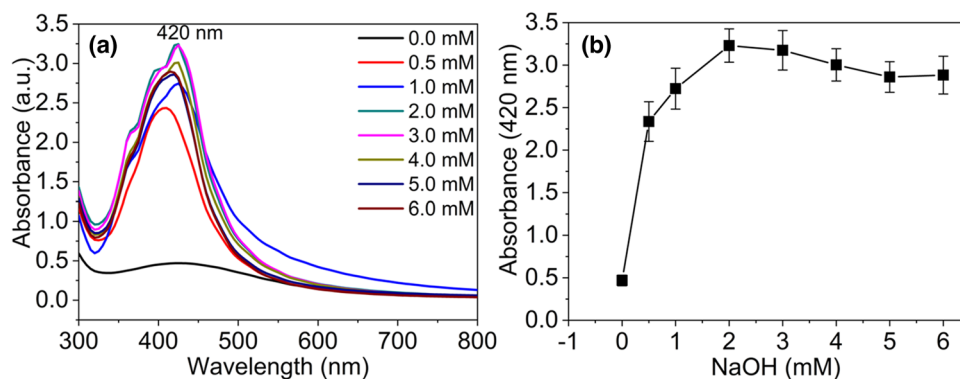
wavelength can be linked to a minor increase in the size or change in density of the AgNPs (Peng et al. 2010). Among the increasing molar ratios of NaOH evaluated, 2 mM NaOH was found to be the optimal concentration, producing the highest yield without compromising the physiochemical properties of the AgNPs—even with an excess of NaOH up to 6 mM (Fig. 1b). These findings underscore the significant role that the presence of a dilute NaOH solution plays in the biosynthetic process. This enables deprotonation of the functional groups in the biomolecules of the cell-free yeast extract, which in turn efficiently reduces $AgNO_3$ and stabilizes the AgNP surfaces, as described by (Jian et al. 2016). The effect of dilute NaOH in the synthesis of AgNPs using this method reveals it is advantageous in tuning the desired classical nucleation and growth route, as reported by (Thanh et al. 2014).

The influence of cell-free yeast extract on the controlling optical properties and yield of AgNPs was explored, as shown in Fig. 2. It displays a single, narrow, and characteristic SPR band with minor shifts, observed at an absorbance wavelength of 420 nm for tested cell-free yeast extract concentrations (Fig. 2a). Notably, the SPR band showed minimal broadening or shifting, which suggests that the optical properties were consistent and that the newly formed AgNPs were in a stable colloidal dispersion. The consistency in the optical properties of AgNPs indicates that cell-free yeast extract plays a vital role in increasing the yield of AgNPs.

The yield of AgNPs showed a linear increase as the concentration of cell-free yeast extract increased. Interestingly, even at higher concentrations of cell-free yeast extract, no adverse effects were observed on either the optical properties or the dispersion of AgNPs. Figure 2b demonstrates an improvement in the absorbance intensity of AgNPs as the cell-free yeast extract concentration ranges from 0.004 to 0.04% (w/v). The highest yield of AgNPs was attained at a relatively low concentration of 0.04% (w/v) of cell-free yeast extract. These results highlight the crucial role of optimal concentration cell-free yeast extract in influencing both the optical properties and the yield of AgNPs. This observation also provides valuable insights into the importance of optimizing reaction parameters for the given biosynthesis process. Such optimization helps in minimizing the generation of byproducts and aligns with the principles of green chemistry (Kim et al. 2017).

Production kinetics of the biosynthesis process was also conducted spectrophotometrically as a function of the metal precursor, $AgNO_3$. Figure 3 displays the minor changes in UV–vis spectra and yield of AgNPs across a range of $AgNO_3$ concentrations. These changes were observed after diluting the reaction sample with DI water in 0.2:0.8 mL. In the concentration spectrum from 0.5 to 1.5 mM of $AgNO_3$, a narrow and characteristic SPR peak appeared at 420 nm (as seen in Fig. 3a). At elevated initial concentrations of $AgNO_3$ between 2 and 3 mM, the SPR band showed a noticeable

Fig. 2 Effect of yeast extract. **a** UV–Vis spectra of AgNPs at increasing initial concentration of cell-free extract of yeast and **b** absorbance intensity of AgNPs suspension at increasing initial concentration of cell-free extract of yeast
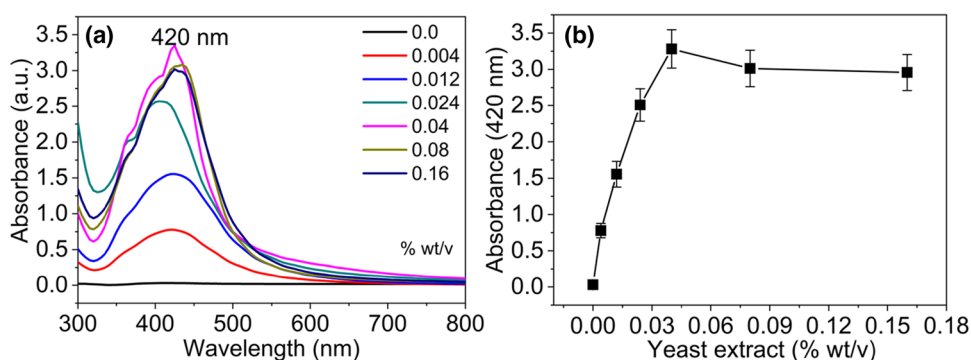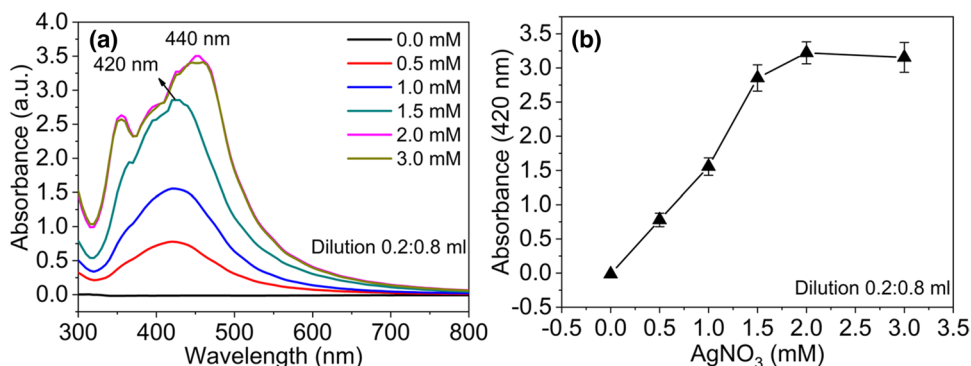
Fig. 3 Effect of $AgNO_3$. **a** UV–Vis spectra of AgNPs at increasing concentration of $AgNO_3$ and **b** absorbance intensity of AgNPs suspension at increasing concentration of $AgNO_3$

shift toward the larger wavelength of about 440 nm. This redshift of 20 nm for the 2 to 3 mM $AgNO_3$ concentrations suggests that an excess of metal precursor results in changes in the size and density of the AgNPs. Absorbance intensity monitored at 420 nm exhibited a linear increase with increasing initial $AgNO_3$ concentration, ranging from 0.5 to 2 mM (Fig. 3b). This linear correlation in the change in absorbance was noted after substantial dilution, indicating successfully achieving high-density suspensions of colloidal AgNPs. Overall, these observations suggest that the AgNPs formed are free from undesirable aggregates as demonstrates isotropic and stable characteristics. These findings offer valuable insights into the efficiency of the developed method for bio-materializing higher initial concentrations of AgNO3, without compromising the desired physicochemical properties of the resulting AgNPs.

Characterization of AgNPs

Adhering to the principles of green chemistry, biosynthesis of AgNPs was conducted using the optimized reaction conditions (NaOH (2 mM), yeast extract (0.05% w/v), and $AgNO_3$ (0.5 mM)). The biosynthesized AgNPs under these optimal conditions were systematically characterized and used for evaluating their antibacterial and seed-priming applications. HR-TEM was employed to investigate the size, shape, and dispersity of the synthesized AgNPs. HR-TEM images revealed that the NPs were nanoscale and exhibited high dispersity, indicating that the synthesis process was well-controlled and yielded uniform AgNPs. As shown in Fig. 4a, the AgNPs predominantly appear in spherical to oval shapes with sizes ranging from 5 to 30 nm. The average size was found to be about ~18 nm. Moreover, the HR-TEM images showcased a high degree of crystallinity within the AgNPs, as evidenced by the presence of well-defined lattice fringes (Fig. 4b). These lattice fringes correspond to the crystallographic planes within the AgNPs structure, further confirming the crystalline nature of the AgNPs. SAED pattern was used to corroborate the crystalline structure of the AgNPs (Fig. 4c). The SAED pattern featured distinct diffraction spots, indicative of the complete reduction of Ag(+) ions to form crystalline Ag(0) NPs. The diffraction pattern also displayed well-defined concentric rings, each corresponds to different sets of crystallographic planes in the AgNPs. In particular, the inner circle is associated with the (111)

Fig. 4 Characterization of **a** HR-TEM image of the biosynthesized AgNPs, **b** Lattice fringe image of the biosynthesized AgNPs, **c** SAED pattern of biosynthesized AgNPs, and **d** XRD spectra of biosynthesized AgNPs
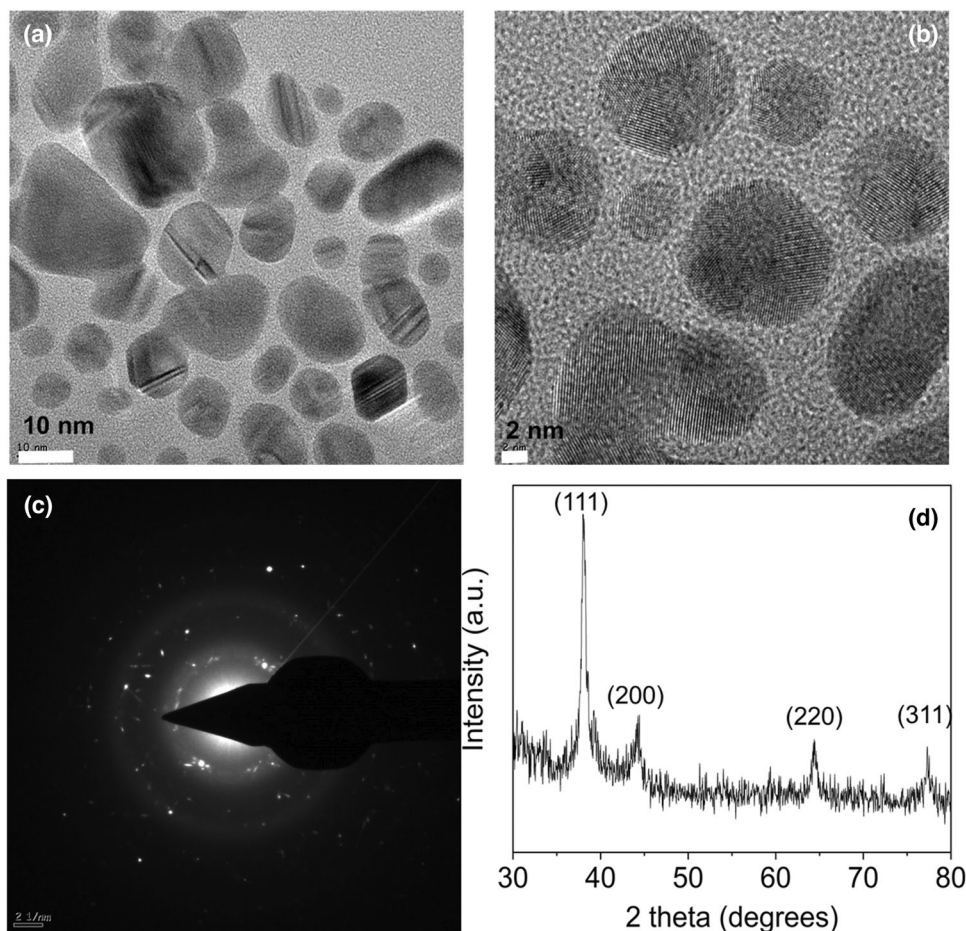
crystallographic orientation, and the external circle aligns with the (311) orientation. The spacing between these concentric rings in the SAED pattern provides important insights into the interatomic distances within the crystal lattice structure of the AgNPs (Fig. 4b, c). These results were further substantiated by XRD spectral analysis, which reinforces the findings from HR-TEM and SAED patterns.

XRD spectral analysis provided valuable insights into the crystal structures and phase composition of the biosynthesized AgNPs. The XRD pattern displayed a series of distinct and well-defined peaks corresponding to specific diffraction angles (2θ). These angles, specifically 38.06°, 44.51°, 64.57°, and 77.28° (as seen in Fig. 4d) were identified from the crystallographic planes as of (111), (200), (220), and (311), respectively. The correlation between the diffraction angles and crystallographic planes is based on their unique positions and intensities within the pattern. One of the striking features of the XRD spectrum was the presence of sharp and well-defined peaks, revealing a high degree of crystallinity within the AgNPs. These results suggest that the high crystallinity of the obtained AgNPs can be a critical factor in determining their physicochemical properties and potential applications. To further look into the characteristics of the biosynthesized AgNPs, the crystallite size was determined using Scherrer's formula for the most prominent peak in the XRD pattern, which corresponds to the (111) plane, yields an estimated crystallite size of about ~ 28 nm. Interestingly, this result correlates with the average particle size (~ 18 nm) revealed from the HR-TEM images (Fig. 4a).

FTIR spectra serve to identify and analyze the functional groups that participate in both the formation and stabilization of AgNPs. In the spectra obtained from the cell-free yeast extract, distinct signature peaks were evident. Specifically, a peak at 3380 cm^{-1} corresponds to the hydroxyl functional groups, while a peak at 1640 was attributed to amide functional groups (as seen in Fig. S1a). However, upon the capping of cell-free yeast extract to the AgNPs, notable changes were observed in the FTIR spectra. One of the most prominent changes was the disappearance of the amide peak at 1640 cm^{-1}, which usually reveals peptide involvement (Kim et al. 2023). The peak in the amide region is generally associated with the vibrations arising from the C=O (carbonyl) symmetric stretching and −NH (amine) asymmetric bending in peptides or proteins (Pérez et al. 2011). The appearance of a prominent peak at 1420 cm^{-1} signifies deprotonation events and suggests enhanced bonding interactions between the peptides from cell-free yeast extract and the surface of AgNPs. Essentially, the shift in this peak could suggest that the yeast extract facilitates the reduction of AgNO$_3$ and stabilizes the AgNPs through surface modification. Additionally, minor changes were observed in the fingerprint region, specifically in the range of 1200 to 800 cm^{-1}. Changes in peak intensities within this region could suggest the involvement of amino acid side chains in stabilizing and interacting with the AgNPs.

The XPS evaluation offered a detailed insight into the constituent elements and their respective chemical states, which include Ag(3d), N(1 s), O(1 s), and C(1 s). Characteristic peaks at distinct electron binding energies were identified as follows: C(1 s) at 284.70 eV, Ag(3d) at 373.39/367.25 eV, N(1 s) at 399.3 eV, and O(1 s) at 531.12 eV (as shown in Fig. S1b). The data relates to Ag3d$_{3/2}$ and Ag3d$_{5/2}$, showing a spin–orbit separation of around 6.14 eV, verifying the successful generation of zero-valent AgNPs (Fig. 5a). The dominant peak for O(1 s) at 531.12 eV, is attributed to the oxygen atoms of deprotonated carbonyl groups (C=O) from the yeast extract that capped the AgNPs (Fig. 5b). A minor peak was noticed at 535.5 eV, which is likely due to the oxygen atoms from hydroxyl groups (–OH) in the side chains of peptides or other biomolecules. Strong peaks for N(1 s) at 399.3 eV and C(1 s) at 284.70 eV further demonstrate the presence of functional groups in peptides that effectively stabilize the AgNP surfaces (refer to Fig. 5c and d).

Antibacterial activity

Herein, we investigated the antibacterial properties of AgNPs against MDR pathogens, specifically *E. coli* (KCCM 11234) and *S. aureus* (KCCM 11335). Turbidity assays were employed to monitor bacterial growth following incubation with AgNPs at varying concentrations ranging from 1 to 20 ppm for preliminary testing and then extending to 20 to 200 ppm for extensive assays, conducted at 37 °C. The data revealed interesting patterns in the antibacterial efficacy of the AgNPs. For *S. aureus*, the results indicated a modest suppression of bacterial growth as the concentration of AgNPs increased within a narrow range (Fig. 6a). A more pronounced reduction in *S. aureus* growth was observed when the concentration reached 50 ppm (50 μg/mL) of AgNPs (Fig. 6b). In contrast, *E. coli* exhibited a stronger sensitivity to AgNPs within identical narrow concentration range (Fig. 6c). Remarkably, complete inhibition of *E. coli* growth was achieved at a concentration of 50 ppm of AgNPs (Fig. 6d). The MIC, the lowest concentration of AgNPs required to inhibit visible bacterial growth, was estimated to be 30 ppm and 50 ppm for *E. coli* and *S. aureus*, respectively. However, negative control exhibited high turbidity, confirming the presence of biosynthesized AgNPs effectively inhibits bacterial growth.

The antibacterial capabilities of AgNPs were examined using the disc diffusion technique. In this method, filter paper discs soaked with varying concentrations of AgNPs were placed onto nutrient agar plates seeded with the target bacteria—either *E. coli* or *S. aureus*. To evaluate the degree of bacterial growth suppression, the plates were incubated

Fig. 5 Core-level XPS spectra of the biosynthesized AgNPs. **a** Ag3d, **b** O1s, **c** N1s, and **d** C1s
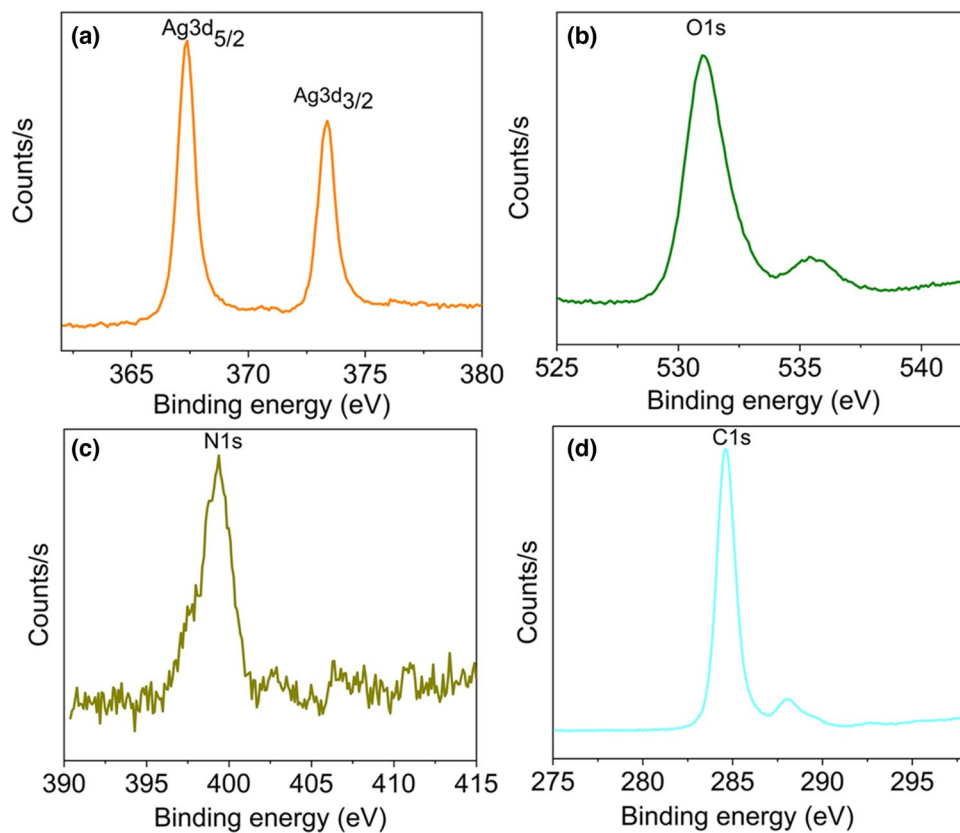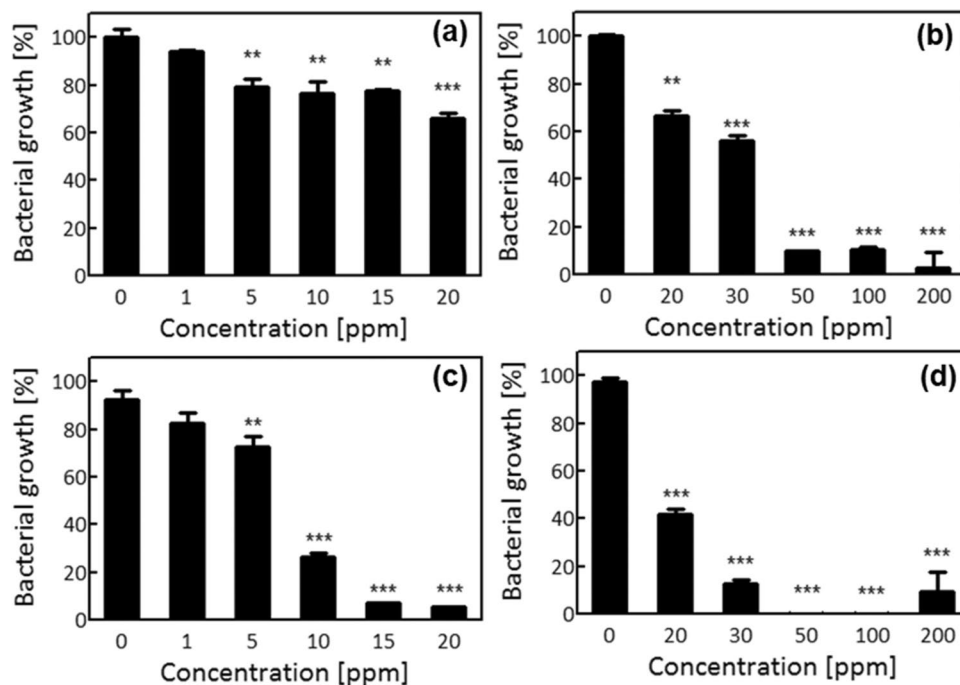
Fig. 6 Cell viability assessed using bacterial growth percentage. **a** and **b** *S. aureus*. **c** and **d** *E. coli*. The antibacterial effect of AgNPs at different concentrations ranging from 1 to 20 ppm and 20 to 200 ppm was compared with control samples (*n* = 3). *Statistically higher activity

at 37 °C and for a 24-h period under static conditions. The absence of visible bacterial growth surrounding the AgNP-impregnated discs served as a clear indicator of the antibacterial efficacy of AgNPs. Figures S2a and b visually compare the zones of inhibition (ZOI) against both tested bacterial strains at different AgNP concentrations, ranging from 10 to 200 ppm. Notably, a trend was observed where the size of the ZOI increased in a concentration-dependent manner.

Among the tested strains, *S. aureus* exhibited a marginally smaller ZOI at each tested dosage of AgNPs when compared to *E. coli*. This could potentially suggest that *E. coli* is more sensitive to AgNPs, possibly due to a mode of action that is particularly effective against gram-negative bacteria. The effectiveness of the tested concentrations of AgNPs in inhibiting bacterial growth was further supported by the findings from the colony count assays.

To further examine the antibacterial efficacy of AgNPs, additional experiments were performed using the colony count assay at varying concentrations of AgNPs. The resulting data, shown in Fig. S3a demonstrate colony count results. Notably, around 65% of *S. aureus* colonies were inhibited at a concentration of 50 ppm of AgNPs, whereas AgNPs reached 100 ppm, and bactericidal efficiency reached near-complete inhibition. In the case of *E. coli*, as shown in Fig. S3b, the bacteria exhibited a very high sensitivity to AgNPs; a 100% killing efficiency was observed at a relatively low concentration of 50 ppm. This sharp decline in bacterial viability suggests that *E. coli* is more susceptible to AgNP treatment at lower concentrations. From the findings, the least amount of AgNPs needed to fully halt bacterial proliferation was determined, referred to as the minimum bactericidal concentration (MBC). For *E. coli*, the MBC was determined to be 50 ppm, whereas for *S. aureus*, it was found to be 100 ppm. These findings are crucial for understanding the optimal concentrations needed for effective antibacterial applications involving AgNPs. These results serve as a standard for comparing the sensitivities of various other bacterial strains to the AgNP treatment, thereby offering valuable insights for both future research and potential clinical applications.

Imaging bacterial morphology

To gain deeper insights into the impact of AgNPs on bacterial morphology, both the *S. aureus* and *E. coli* cells were treated with a 30 ppm concentration of AgNPs and then subjected to Gram staining and microscopic examination. In the untreated control groups, both bacterial species maintained their typical morphologies; *S. aureus* cells appeared dark violet, indicative of an intact, gram-positive cell wall, while E. coli cells appeared pink, suggesting an intact, gram-negative cell membrane (Fig. S4a and b). However, upon treatment with AgNPs, morphological changes were observed in both bacterial types. For *S. aureus*, cells treated with AgNPs showed substantial aggregates, likely indicating cell death. Moreover, the cellular debris scattered around aggregates appeared in shades of pale yellow and blue, contrasting the sharp dark violet color of healthy, untreated cells (Fig. S4c). On the other hand, the *E. coli* cells presented a different set of morphological changes upon AgNP treatment. Unlike the dark pink color of the untreated cells, which is indicative

of healthy, gram-negative membranes, the AgNP-treated *E. coli* cells, showed a much pale coloration. This suggests that in the presence of AgNPs, bacterial cells experience compromised membrane integrity, which could potentially lead to cell death or significant cellular stress (Fig. S4b and d).

The use of FESEM offered a more clear perspective on the bactericidal action of AgNPs at the cellular level. In the control samples, *S. aureus* cells exhibited their typical, spherical morphology, complete with smooth, intact cell walls (Fig. 7a). These images served as baselines for assessing the extent of cell damage post-AgNPs exposure. In contrast, the *S. aureus* cells treated with 30 ppm of AgNPs showed severely compromised cell walls, irregular broken cell membranes, and other forms of damage (Fig. 7b). This led to a noticeable change in the size and shape of cells, with apparent cytoplasm leakage, suggesting the likely collapse internal osmotic balance of the bacterial cells. *E. coli* cells in the control group also presented their characteristic rod-like shape and healthy cell walls (Fig. 7c). FESEM images of *E. coli* exposed to AgNPs were evident of damaged and fractured cell walls (Fig. 7d). Like *S. aureus*, these cells also displayed severe membrane damage and deformities. The formerly smooth and rod-shaped *E. coli* cells transform into physically disrupted structures, suggesting that AgNPs exert their antibacterial effects by compromising cell membrane integrity, which leads to either bacterial cell death or significant cellular stress.

Seed priming results

The study further extended its focus to explore the applications of AgNPs beyond their antibacterial properties, particularly investigating their potential as nano-priming agents in agriculture. Two model crops were chosen for the investigation—*Sorghum jowar* and *Zea mays*. The goal was to assess whether AgNPs could enhance seed germination rates and seedling vigor. Compared to the control group (unprimed seeds), seeds primed with AgNPs (10 to 70 ppm) displayed a higher mean germination time and germination rate for both crop types. This highlights the effectiveness of AgNPs as nano-priming agents in enhancing the germination process. Specifically, in *Sorghum jowar*, seeds treated with 30 ppm of AgNPs showed a substantial improvement in germination performance. As indicated in Fig. 8a, these seeds germinated faster than those in the control group. When the concentration of AgNPs was increased to 40 ppm, the seeds achieved a 50% germination rate in a significantly shorter period and maximum seed germination percentage compared to the control group (Fig. 8a). The average seed germination percentages for *Sorghum jowar* seeds treated with 50 ppm, 60 ppm, and 70 ppm of AgNPs were 95%, 94%, and 96%, respectively. These rates are comparatively positive to a germination rate of about 63% observed in the non-primed

Fig. 7 FESEM imaging. **a** Control *S. aureus* cells, **b** AgNP-treated *S. aureus* cells, **c** control *E. coli* cells, and **d** AgNP-treated *E. coli* cells
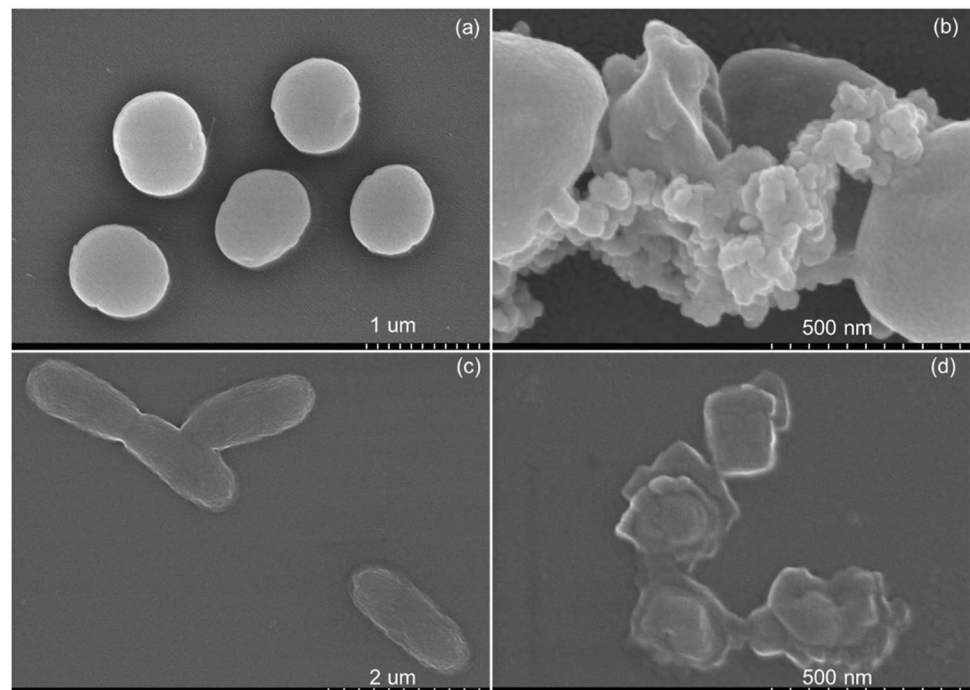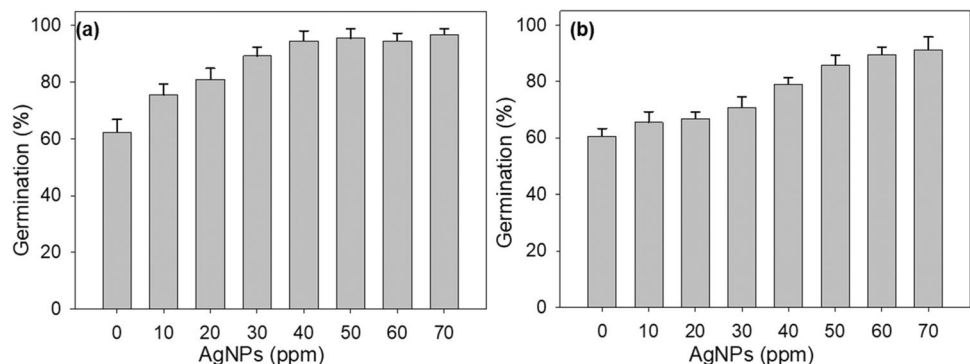

Fig. 8 Effect of nano-priming on seed germination percentage. Germination of **a** *Sorghum jowar* seeds and **b** *Zea mays* seeds

seeds. These results demonstrate the effectiveness of AgNPs as nano-priming agents in the range of the tested concentrations. Firstly, AgNPs, at relatively low concentrations, can act as effective seed priming agents, enhancing the overall efficiency of seed germination. Secondly, the data indicates that even a slight increase in the AgNP concentration (from 30 to 40 ppm in this case) can make a noticeable difference in the speed and percentage of germination, pointing to a concentration-dependent effect.

The investigation into the potential of AgNPs as seed priming agents also involved experiments with *Zea mays*. Similar to the findings in *Sorghum jowar*, the study found that the germination of *Zea mays* seeds was also enhanced through AgNP priming. A concentration-dependent effect was not observed, confirming that the AgNPs play a pivotal role in influencing seed germination rates. Specifically, when the *Zea mays* seeds were treated with 60 ppm and 70 ppm

concentrations of AgNPs, the germination percentage reached the maximum. This is a significant boost, especially when compared to the germination percentage of non-treated seeds, which was only around 60% (as indicated in Fig. 8b). It is worth noting that while the overall seedling growth was comparable between the primed and unprimed seeds, the germination percentage was improved in the AgNP-primed group. One of the critical outcomes of this study was the absence of any observable toxicity at the tested concentrations of AgNPs. This suggests that the use of AgNPs as nano-priming agents is likely to be a safe practice under the tested concentrations. The results suggest nano-priming technique has the potential to act as a protective measure against seed-borne pathogens and diseases, thereby serving as a two-fold benefit—improved germination and crop protection. Further research and real-world application of NP-based seed priming approaches are advised to maximize

the benefits of promising nanotechnological innovations in modern agricultural practices.

Discussion

The optimization of reaction parameters—such as pH, yeast extract concentration, and the $AgNO_3$ precursor ratio—was systematically investigated using UV–vis spectroscopy. This optimization aimed to identify the most favorable conditions that would maximize the yield of AgNPs while minimizing the formation of undesirable by-products. Implementation of green chemistry principles and careful selection of the reaction parameters successfully achieved efficient biosynthesis of AgNPs with improved physicochemical characteristics (Liaqat et al. 2022). The decision to employ elevated temperature and alkaline conditions was driven by the goal of following the classical nucleation and growth route, which has been proven beneficial in previous studies (Naik et al. 2019; Thanh et al. 2014). This strategy eases the production of desired AgNPs minimizes waste generation and avoids the need for solvent-intensive purification steps. These results are consistent with the principles of safer and more sustainable methods for synthesizing antibacterial AgNPs, as suggested by other research (Ajitha et al. 2019). The successful adoption of eco-friendly synthesis strategies highlights the potential of our method as a greener alternative for producing both antibacterial and seed priming agents.

The influence of alkaline conditions on the biosynthesis of AgNPs was examined by varying NaOH concentrations between 0.5 and 6 mM. The data revealed a clear dependency of AgNP synthesis on the addition of dilute NaOH (Fig. 1a). Importantly, even at elevated NaOH concentrations ranging from 3 to 6 mM, only minor reductions in absorbance intensities were observed. This suggests that the physicochemical properties of the AgNPs remained largely unaffected (Fig. 1b). These findings indicate that dilute NaOH plays a vital role in facilitating AgNP synthesis by promoting the deprotonation of functional groups in the yeast extract biomolecules. Such deprotonation enables the enhanced reduction of Ag ions and stabilizes the newly formed AgNPs, as documented by a previous study (Axson et al. 2015). The deprotonated states of amine, hydroxyl, and carboxyl acid groups under neutral or alkaline conditions are known to enhance AgNP surface passivation, leading to the formation of a stable colloidal dispersion through electrostatic repulsion (Kim et al. 2018; Yang et al. 2016). Our qualitative and quantitative results regarding the addition of dilute NaOH align well with literature findings (Darroudi et al. 2010), further supporting the critical role of NaOH in the successful synthesis of AgNPs.

The influence of yeast extract concentration in the biosynthesis of AgNPs was methodically investigated. In these tests, the ratio of $AgNO_3$ to NaOH was held constant to identify the effects of the yeast extract. Utilizing absorbance data from UV–visible spectroscopy, the yield of AgNPs is strictly dependent on the amount of yeast extract used in the reaction (refer to Fig. 2a and b). Interestingly, the data revealed that achieving a high yield of AgNPs does not demand an excessive amount of yeast extract. In particular, it was found that the maximum yield can be achieved at a substantially low concentration range of yeast extract (as seen in Fig. 2b). This noteworthy finding suggests that the developed green method is an economical and efficient route for metal NP synthesis as it suits to implement atom economy principle of green chemistry (Soltys et al. 2021). Moreover, the consistency in the SPR bands for various yeast extract concentrations indicates a high degree of uniformity in the AgNPs synthesized, including various parameters such as size, shape, and morphological characteristics, as well as dielectric environment and elemental composition (Liaqat et al. 2022). This is a significant observation, suggesting that the cell-free extract yeast allows for finding a reliable system for the production of high-quality AgNPs. UV–visible spectra as an analytical tool can be instrumental for both qualitative and quantitative assessments of metal NP synthesis under different reaction parameters (Kim et al. 2016). This parameter assisted in identifying the optimal concentration of yeast extract for AgNP synthesis and highlighted the potential for achieving high-quality, uniform AgNPs efficiently and sustainably.

The production kinetics of AgNPs using this method were evaluated at varying initial concentrations of the $AgNO_3$ metal precursor. The data showed that the highest yield of AgNPs occurred at a concentration of 2 mM $AgNO_3$ (see Fig. 3a and b). This result suggests that the biosynthetic approach is highly suitable for establishing high-concentration suspensions of AgNPs, indicating its substantial potential for scaled-up manufacturing. The intensity of the absorbance for the AgNPs solution at its SPR peak was found to be proportional to the concentration of the AgNPs (Abkhalimov et al. 2022). This parameter is highly relevant as it aligns with fundamental tenets of green chemistry and engineering, including the use of eco-friendly solvents, renewable raw materials, safer chemical processes, and efficient use of resources (Dahl et al. 2007). Therefore, optimizing synthesis parameters for a given method is vital for establishing commercial manufacturing processes that maximize the conversion of precursor reagents into the desired nanoproducts (Freund et al. 2018).

After synthesizing the AgNPs, various characterization techniques were employed to examine their physicochemical properties, including HR-TEM, XRD, FTIR, and XPS. HR-TEM imaging revealed that the AgNPs exhibit shapes ranging from spherical to oval, and their formation follows classical nucleation and isotropic growth route. The AgNPs were

found to have a size range between 5 and 30 nm, which is known for conferring unique physicochemical properties like a higher surface-to-volume ratio. These characteristics make them valuable for applications in sensing, catalysis, and the biomedical field (Riaz et al. 2022). SAED pattern displayed in the HR-TEM images indicated the presence of different orientations and crystal planes, suggesting that the synthesized AgNPs have a face-centered cubic (fcc) structure (see Fig. 4c). The size range and morphologies of the AgNPs observed in this study align well with previous reports on the biosynthesis of AgNPs (Rodríguez-Serrano et al. 2020; Tekin et al. 2019), further validating the significance of our biosynthetic method.

The XRD spectra of biosynthesized AgNPs were found to be in accord with the standard (JCPDS file no. 03–0921) and found to agree with the face-centered cubic (FCC) crystalline structures of Ag(0) (Zaman et al. 2023). XRD findings of the AgNPs show the presence of diffraction planes corresponding to the (111), (200), (220), and (311) planes. This XRD analysis provides evidence that the cell-free yeast extract effectively reduces Ag(+) ions to Ag(0) and stabilizes the newly formed crystalline AgNPs. Additionally, the pattern included some unassigned peaks with minor intensity, suggesting the presence of bioorganic compounds on the AgNP surfaces (Anandalakshmi et al. 2016). These findings are consistent with a referenced report (Khanal et al. 2022), further validating the effectiveness of the biosynthesis method.

FTIR analysis was used to investigate the functional groups and interactions between cell-free yeast extract molecules and AgNPs. The presence of intense peaks in the FTIR spectra is associated with carboxylate (COO−) groups indicating that these surface functional groups bond to the AgNPs (Fig. S1a), and contribute to the excellent stability of the AgNP dispersion. The FTIR results indicate that cell-free yeast extract contains a variety of functional groups. Changes observed in the spectra upon interaction with AgNPs suggest that these functional groups undergo modifications and interactions, highlighting their role in stabilizing the AgNPs (Piotrowska and Masek 2015).

Additionally, XPS was employed to examine the surface chemistry and elemental composition of yeast extract-AgNPs. The core-level XPS spectra for Ag(3d) showed two distinct peaks at 373.39 eV for $Ag3d_{3/2}$ and 367.25 eV for $Ag3d_{5/2}$ with the spin–orbit split of about 6.14 eV (Fig. 5a), reveals the formation of zero-valent silver (Shu et al. 2020). The core-level XPS spectra of C(1 s) displayed an intense peak (Fig. 5d), indicating the effective capping of AgNPs through the carboxyl functional groups of the peptides present in yeast extract (Nguyen et al. 2005). FTIR and XPS results together suggest the likely formation of molecular interactions and robust functionalization of the AgNPs. These findings support the potential application of

biosynthesized AgNPs in various fields, including biomedicine, antibacterial, and seed priming.

After the biosynthesis and characterization of AgNPs, it is confirmed that this method is appropriate for producing high-density suspensions of the desired AgNPs. The antibacterial properties of the AgNPs were assessed using different assays, to identify potent antibacterial efficacy, particularly against MDR bacteria. The assessment of bacterial viability and bactericidal activity assessed by turbidity and colony count assays supported the strong antibacterial activity of AgNPs. Our findings align with previous reports showing that AgNPs exhibit higher sensitivity against gram-negative than gram-positive owing to differences in their cell wall components and membrane structures (Dakal et al. 2016). The observed antibacterial efficacy is attributed to the unique characteristics of biosynthesized AgNPs, including narrow size distribution, high dispersity, and enhanced colloidal stability (Ferreira et al. 2023). Such intrinsic properties of the biosynthesized AgNPs make them excellent candidates as potent antibacterial agents, with great potential for various biomedical applications (Shao et al. 2015).

The combination of gram staining and FE-SEM was used for visualizing the morphological changes induced by AgNPs, providing clear evidence of their potential as effective antibacterial agents. The gram staining results revealed the formation of cellular debris, highlighting the potential use of AgNPs in eradicating biofilms and in the development of alternative antibacterial agents to MDR bacterial pathogens (Kumar et al. 2023a). Utilizing gram staining and optical microscopy, morphological changes were observed and confirmed the antibacterial efficacy of the biosynthesized AgNPs against the tested bacteria (Ghodake et al. 2020a). The nanoscale alterations to the integrity of bacterial cell walls and membranes after treatment with AgNPs were further validated by FE-SEM. Through FE-SEM, mechanistic insights were gained into the mode of action of AgNPs by imaging the morphological changes in AgNP-treated *S. aureus* and *E. coli* cells. The results suggest that AgNPs exert a strong influence on the cell walls of bacterial pathogens, leading to the collapse of their integrity and the formation of cell debris aggregates (Qing et al. 2018).

The irreversible structural damage inflicted by AgNPs on bacterial cells is likely responsible for inducing apoptosis, as evidenced by the observed physical damage phenomena (Rasool et al. 2016). This kind of mechanism of action could contribute to the development of alternative antibacterial agents that effectively combat MDR pathogens. The proposed antibacterial mechanism of AgNPs involves several steps. First, yeast extract nutrients and the excellent colloidal dispersion of AgNPs allows bacterial cells to attract toward the AgNPs' surface and form electrostatic interactions with components in bacterial cell walls (Joshi et al. 2020). Subsequently, the AgNPs, along with released Ag ions, cause

physical damage to the bacterial cells (López-Heras et al. 2015), leading to the excessive generation of reactive oxygen species (Mammari et al. 2022), loss of cellular integrity (Su et al. 2009), and cytoplasmic leakage (Qing et al. 2018). This multifaceted mode of action highlights the potential of AgNPs as efficient antibacterial agents and demands advancing investigation in the development of novel strategies to combat antibiotic resistance and infectious diseases (Ribeiro et al. 2022).

The application of biosynthesized AgNPs in seed priming for *Sorghum jowar* and *Zea mays* seeds has been demonstrated to enhance seed germination, seedling vigor, and disease resistance. This finding suggests that AgNP-based seed priming holds considerable potential for practical use by farmers, as it improves crop performance and reduces the time and costs associated with fertilizers, re-sowing, and substituting weak plantlets (Sundaria et al. 2019). Our previous work has shown that nano-priming technology is emerging as a more effective practice compared to conventional agrochemical-based seed priming methods (Nile et al. 2022). Various types of metal nanoparticles, such as gold NPs (Venzhik et al. 2022), copper NPs (Faraz et al. 2023), iron NPs (Panyuta et al. 2016), TiO_2 NPs (Shah et al. 2021), zinc NPs (Taran et al. 2017), and carbon-based nanomaterials (Krumova et al. 2023), have been explored as potential seed treatment or priming agents. These agents have been applied to enhance the germination rate, seedling growth, and stress tolerance in a wide range of crops. Therefore, nanotechnology-based seed priming offers an improvement in current agricultural practices by providing farmers with low-cost, reliable, and efficient tools for establishing healthy and robust crops. The observed germination results in this study seem in agreement with a previous report that has demonstrated enhanced germination rates for crops such as *Citrullus lanatus*, *Cucurbita zucchini*, and *Zea mays* at different AgNP concentrations (Almutairi and Alharbi 2015). Similarly, the priming of aged rice seeds with phytosynthesized AgNPs showed a significant improvement in germination rate, disease-free roots, and better seedling vigor compared to the non-primed control group (Mahakham et al. 2017). In conclusion, the use of AgNPs seed priming agent presents a promising and sustainable approach to enhancing agricultural productivity. Further research and implementation of AgNP-based antibacterial and seed priming agents hold great potential for positively impacting global agriculture and ensuring food security in the face of changing environmental challenges.

Supplementary Information The online version contains supplementary material available at https://doi.org/10.1007/s00253-023-12920-7.

Author contribution Conceptualization, D-Y.K. and J-S.S.; methodology, M.K., J-S.S., A.S., and G.S.G.; nanoparticle preparation and characterization, G.S.G. and A.S.; antibacterial investigation, G.S.G., M.K., and J-S.S.; formal analysis, S.N., J.R.K., C.S.S., and A.S.; data curation, M.K., J.R.K., C.S.S., and S.N.; supervision, D-Y.K., J-S.S., S.N., and A.H.B.; validation, D-Y.K., J-S.S., C.S.S., and A.H.B.; writing—original draft, D-Y.K. and G.S.G.; writing—review and editing, D-Y.K., J-S.S., M.K., J.R.K., S.N., A.S., A.H.B., C.S.S., and G.S.G. All authors have reviewed the manuscript and approved the submission of the manuscript.

Data availability Research data will be available upon request to the corresponding author.

Declarations

Ethics approval This article does not contain any studies with human participants or animals performed by any of the authors.

Conflict of interest The authors declare no competing interests.

References

Abkhalimov E, Ershov V, Ershov B (2022) Determination of the concentration of silver atoms in hydrosol nanoparticles. Nanomaterials 12(18):3091. https://doi.org/10.3390/nano12183091

Acharya P, Jayaprakasha GK, Crosby KM, Jifon JL, Patil BS (2020) Nanoparticle-mediated seed priming improves germination, growth, yield, and quality of watermelons (Citrullus lanatus) at multi-locations in Texas. Sci Rep 10(1):5037. https://doi.org/10.1038/s41598-020-61696-7

Adebisi YA (2023) Balancing the risks and benefits of antibiotic use in a globalized world: the ethics of antimicrobial resistance. Glob Health 19(1):27. https://doi.org/10.1186/s12992-023-00930-z

Agreles MAA, Cavalcanti IDL, Cavalcanti IMF (2022) Synergism between metallic nanoparticles and antibiotics. Appl Microbiol Biotechnol 106(11):3973–3984. https://doi.org/10.1007/s00253-022-12001-1

Ajitha B, Reddy YAK, Lee Y, Kim MJ, Ahn CW (2019) Biomimetic synthesis of silver nanoparticles using Syzygium aromaticum (clove) extract: catalytic and antimicrobial effects. Appl Organomet Chem 33(5):e4867. https://doi.org/10.1002/aoc.4867

Ali A, Ovais M, Cui X, Rui Y, Chen C (2020) Safety assessment of nanomaterials for antimicrobial applications. Chem Res Toxicol 33(5):1082–1109. https://doi.org/10.1021/acs.chemrestox.9b00519

Almutairi Z, Alharbi A (2015) Effect of silver nanoparticles on seed germination of crop plants. J Adv Agric 4(1):280–285. https://doi.org/10.24297/jaa.v4i1.4295

Altarac D, Gutch M, Mueller J, Ronsheim M, Tommasi R, Perros M (2021) Challenges and opportunities in the discovery, development, and commercialization of pathogen-targeted antibiotics. Drug Discov Today 26(9):2084–2089. https://doi.org/10.1016/j.drudis.2021.02.014

Anandalakshmi K, Venugobal J, Ramasamy V (2016) Characterization of silver nanoparticles by green synthesis method using Pedalium murex leaf extract and their antibacterial activity. Appl Nanosci 6(3):399–408. https://doi.org/10.1007/s13204-015-0449-z

Arif R, Uddin R (2021) A review on recent developments in the biosynthesis of silver nanoparticles and its biomedical applications. Med Devices Sens 4(1):e10158. https://doi.org/10.1002/mds3.10158

Augustine R, Hasan A, Primavera R, Wilson RJ, Thakor AS, Kevadiya BD (2020) Cellular uptake and retention of nanoparticles: insights on particle properties and interaction with cellular components. Mater Today Commun 25:101692. https://doi.org/10.1016/j.mtcomm.2020.101692

Axson JL, Stark DI, Bondy AL, Capracotta SS, Maynard AD, Philbert MA, Bergin IL, Ault AP (2015) Rapid kinetics of size and pH-dependent dissolution and aggregation of silver nanoparticles in simulated gastric fluid. J Phys Chem C 119(35):20632–20641. https://doi.org/10.1021/acs.jpcc.5b03634

Ayukekbong JA, Ntemgwa M, Atabe AN (2017) The threat of antimicrobial resistance in developing countries: causes and control strategies. Antimicrob Resist Infect Control 6(1):47. https://doi.org/10.1186/s13756-017-0208-x

Bahrulolum H, Nooraei S, Javanshir N, Tarrahimofrad H, Mirbagheri VS, Easton AJ, Ahmadian G (2021) Green synthesis of metal nanoparticles using microorganisms and their application in the agrifood sector. J Nanobiotechnol 19(1):86. https://doi.org/10.1186/s12951-021-00834-3

Bano N, Iqbal D, Al Othaim A, Kamal M, Albadrani HM, Algehainy NA, Alyenbaawi H, Alghofaili F, Amir M, Roohi, (2023) Antibacterial efficacy of synthesized silver nanoparticles of Microbacterium proteolyticum LA2(R) and Streptomyces rochei LA2(O) against biofilm forming meningitis causing microbes. Sci Rep 13(1):4150. https://doi.org/10.1038/s41598-023-30215-9

Chakraborty N, Jha D, Roy I, Kumar P, Gaurav SS, Marimuthu K, Ng O-T, Lakshminarayanan R, Verma NK, Gautam HK (2022) Nanobiotics against antimicrobial resistance: harnessing the power of nanoscale materials and technologies. J Nanobiotechnol 20(1):375. https://doi.org/10.1186/s12951-022-01573-9

Dadgostar P (2019) Antimicrobial resistance: implications and costs. Infect Drug Resist 12:3903–3910. https://doi.org/10.2147/idr.S234610

Dahl JA, Maddux BLS, Hutchison JE (2007) Toward greener nanosynthesis. Chem Rev 107(6):2228–2269. https://doi.org/10.1021/cr050943k

Dakal TC, Kumar A, Majumdar RS, Yadav V (2016) Mechanistic basis of antimicrobial actions of silver nanoparticles. Front Microbiol 7:1831. https://doi.org/10.3389/fmicb.2016.01831

Darroudi M, Ahmad MB, Abdullah AH, Ibrahim NA, Shameli K (2010) Effect of accelerator in green synthesis of silver nanoparticles. Int J Mol Sci 11(10):3898–3905. https://doi.org/10.3390/ijms11103898

Deshmukh SP, Patil SM, Mullani SB, Delekar SD (2019) Silver nanoparticles as an effective disinfectant: a review. Mater Sci Eng: C 97:954–965. https://doi.org/10.1016/j.msec.2018.12.102

Faraz A, Faizan M, Rajput VD, Minkina T, Hayat S, Faisal M, Alatar AA, Abdel-Salam EM (2023) CuO nanoparticle-mediated seed priming improves physio-biochemical and enzymatic activities of Brassica juncea. Plants 12(4):803

Ferreira AM, Vikulina A, Loughlin M, Volodkin D (2023) How similar is the antibacterial activity of silver nanoparticles coated with different capping agents? RSC Adv 13(16):10542–10555. https://doi.org/10.1039/D3RA00917C

Freund R, Lächelt U, Gruber T, Rühle B, Wuttke S (2018) Multifunctional efficiency: extending the concept of atom economy to functional nanomaterials. ACS Nano 12(3):2094–2105. https://doi.org/10.1021/acsnano.8b00932

Garg P, Attri P, Sharma R, Chauhan M, Chaudhary GR (2022) Advances and perspective on antimicrobial nanomaterials for biomedical applications. Front Nanotechnol 4:898411. https://doi.org/10.3389/fnano.2022.898411

Ghodake G, Kim M, Sung J-S, Shinde S, Yang J, Hwang K, Kim D-Y (2020a) Extracellular synthesis and characterization of silver nanoparticles—antibacterial activity against multidrug-resistant bacterial strains. Nanomaterials 10(2):360. https://doi.org/10.3390/nano10020360

Ghodake G, Shinde S, Saratale GD, Kadam A, Saratale RG, Kim D-Y (2020b) Water purification filter prepared by layer-by-layer assembly of paper filter and polypropylene-polyethylene woven fabrics decorated with silver nanoparticles. Fibers and Polym 21(4):751–761. https://doi.org/10.1007/s12221-020-9624-2

Ghosh S, Ahmad R, Zeyaullah M, Khare SK (2021) Microbial nanofactories: synthesis and biomedical applications. Front Chem 9:626834. https://doi.org/10.3389/fchem.2021.626834

Heuer-Jungemann A, Feliu N, Bakaimi I, Hamaly M, Alkilany A, Chakraborty I, Masood A, Casula MF, Kostopoulou A, Oh E, Susumu K, Stewart MH, Medintz IL, Stratakis E, Parak WJ, Kanaras AG (2019) The role of ligands in the chemical synthesis and applications of inorganic nanoparticles. Chem Rev 119(8):4819–4880. https://doi.org/10.1021/acs.chemrev.8b00733

Hochvaldová L, Večeřová R, Kolář M, Prucek R, Kvítek L, Lapčík L, Panáček A (2022) Antibacterial nanomaterials: upcoming hope to overcome antibiotic resistance crisis. Nanotechnol Rev 11(1):1115–1142. https://doi.org/10.1515/ntrev-2022-0059

Hulkoti NI, Taranath TC (2014) Biosynthesis of nanoparticles using microbes—a review. Colloids Surf b: Biointerfaces 121:474–483. https://doi.org/10.1016/j.colsurfb.2014.05.027

Iravani S, Korbekandi H, Mirmohammadi SV, Zolfaghari B (2014) Synthesis of silver nanoparticles: chemical, physical and biological methods. Res Pharm Sci 9(6):385–406

Jian W, Zhang L, Siu KC, Song A, Wu JY (2016) Formation and physiochemical properties of silver nanoparticles with various exopolysaccharides of a medicinal fungus in aqueous solution. Molecules 22(1):50. https://doi.org/10.3390/molecules22010050

Joshi AS, Singh P, Mijakovic I (2020) Interactions of gold and silver nanoparticles with bacterial biofilms: molecular interactions behind inhibition and resistance. Int J Mol Sci 21(20):7658. https://doi.org/10.3390/ijms21207658

Khanal L, Sharma K, Paudyal H, Parajuli K, Dahal B, Gc G, Pokharel Y, Kalauni S (2022) Green Synthesis of silver nanoparticles from root extracts of Rubus ellipticus sm. and comparison of antioxidant and antibacterial activity. J Nanomater 2022:1–11. https://doi.org/10.1155/2022/1832587

Kim H-s, Seo YS, Kim K, Han JW, Park Y, Cho S (2016) Concentration effect of reducing agents on green synthesis of gold nanoparticles: size, morphology, and growth mechanism. Nanoscale Res Lett 11(1):230. https://doi.org/10.1186/s11671-016-1393-x

Kim D-Y, Kim M, Shinde S, Saratale RG, Sung J-S, Ghodake G (2017) Temperature dependent synthesis of tryptophan-functionalized gold nanoparticles and their application in imaging human neuronal cells. ACS Sustain Chem Eng 5(9):7678–7689. https://doi.org/10.1021/acssuschemeng.7b01101

Kim D-Y, Saratale RG, Shinde S, Syed A, Ameen F, Ghodake G (2018) Green synthesis of silver nanoparticles using Laminaria japonica extract: characterization and seedling growth assessment. J Clean Prod 172:2910–2918. https://doi.org/10.1016/j.jclepro.2017.11.123

Kim D-Y, Sharma SK, Rasool K, Koduru JR, Syed A, Ghodake G (2023) Development of novel peptide-modified silver nanoparticle-based rapid biosensors for detecting aminoglycoside antibiotics. J Agric Food Chem 71(34):12883–12898. https://doi.org/10.1021/acs.jafc.3c03565

Krumova S, Petrova A, Petrova N, Stoichev S, Ilkov D, Tsonev T, Petrov P, Koleva D, Velikova V (2023) Seed priming with single-walled carbon nanotubes grafted with pluronic p85 preserves the functional and structural characteristics of pea plants. Nanomaterials 13(8):1332. https://doi.org/10.3390/nano13081332

Kumar L, Bisen M, Harjai K, Chhibber S, Azizov S, Lalhlenmawia H, Kumar D (2023a) Advances in nanotechnology for biofilm

inhibition. ACS Omega 8(24):21391–21409. https://doi.org/10.1021/acsomega.3c02239

Kumar M, Silori R, Mazumder P, Shrivastava V, Loge F, Barceló D, Mahlknecht J (2023b) Wars and pandemics: AMR accelerators of the 21st century? Environmen Sci Technol Lett 10(4):289–291. https://doi.org/10.1021/acs.estlett.3c00020

Lethongkam S, Sunghan J, Wangdee C, Durongphongtorn S, Siri R, Wunnoo S, Paosen S, Voravuthikunchai SP, Dejyong K, Daengngam C (2023) Biogenic nanosilver-fabricated endotracheal tube to prevent microbial colonization in a veterinary hospital. Appl Microbiol Biotechnol 107(2):623–638. https://doi.org/10.1007/s00253-022-12327-w

Liaqat N, Jahan N, Khalil-ur-Rahman AT, Qureshi H (2022) Green synthesized silver nanoparticles: optimization, characterization, antimicrobial activity, and cytotoxicity study by hemolysis assay. Front Chem 10:952006. https://doi.org/10.3389/fchem.2022.952006

López-Heras M, Theodorou IG, Leo BF, Ryan MP, Porter AE (2015) Towards understanding the antibacterial activity of Ag nanoparticles: electron microscopy in the analysis of the materials-biology interface in the lung. Environ Scie: Nano 2(4):312–326. https://doi.org/10.1039/C5EN00051C

Mahakham W, Sarmah AK, Maensiri S, Theerakulpisut P (2017) Nanopriming technology for enhancing germination and starch metabolism of aged rice seeds using phytosynthesized silver nanoparticles. Sci Rep 7(1):8263. https://doi.org/10.1038/s41598-017-08669-5

Mammari N, Lamouroux E, Boudier A, Duval RE (2022) Current knowledge on the oxidative-stress-mediated antimicrobial properties of metal-based nanoparticles. Microorganisms 10(2):437. https://doi.org/10.3390/microorganisms10020437

Naik AN, Patra S, Sen D, Goswami A (2019) Evaluating the mechanism of nucleation and growth of silver nanoparticles in a polymer membrane under continuous precursor supply: tuning of multiple to single nucleation pathway. Phy Chem Chem Phy 21(8):4193–4199. https://doi.org/10.1039/C8CP06202A

Nguyen TKT, Victor FP, Le DT, David GF (2005) Peptides as capping ligands for in situ synthesis of water soluble Co nanoparticles for bioapplications. J Phys Conf Ser 17(1):70. https://doi.org/10.1088/1742-6596/17/1/012

Nile SH, Thiruvengadam M, Wang Y, Samynathan R, Shariati MA, Rebezov M, Nile A, Sun M, Venkidasamy B, Xiao J, Kai G (2022) Nano-priming as emerging seed priming technology for sustainable agriculture—recent developments and future perspectives. J Nanobiotechnol 20(1):254. https://doi.org/10.1186/s12951-022-01423-8

Noorafsha KAK, Kashyap A, Deshmukh L, Vishwakarma D (2022) Biosynthesis and biophysical elucidation of CuO nanoparticle from Nyctanthes arbor-tristis Linn leaf. Appl Microbiol Biotechnol 106(17):5823–5832. https://doi.org/10.1007/s00253-022-12105-8

Pallavicini P, Dacarro G (2018) Taglietti A (2018) Self-assembled monolayers of silver nanoparticles: from intrinsic to switchable inorganic antibacterial surfaces. Eur J Inorg Chem 45:4846–4855. https://doi.org/10.1002/ejic.201800709

Panyuta O, Belava V, Fomaidi S, Kalinichenko O, Volkogon M, Taran N (2016) The effect of pre-sowing seed treatment with metal nanoparticles on the formation of the defensive reaction of wheat seedlings infected with the eyespot causal agent. Nanoscale Res Lett 11(1):92. https://doi.org/10.1186/s11671-016-1305-0

Peng S, McMahon JM, Schatz GC, Gray SK, Sun Y (2010) Reversing the size-dependence of surface plasmon resonances. Proc Natl Acad Sci 107(33):14530–14534. https://doi.org/10.1073/pnas.1007524107

Pérez Y, Mann E, Herradón B (2011) Preparation and characterization of gold nanoparticles capped by peptide–biphenyl hybrids.

J Colloid and Interface Sci 359(2):443–453. https://doi.org/10.1016/j.jcis.2011.04.029

Piotrowska M, Masek A (2015) Saccharomyces cerevisiae cell wall components as tools for ochratoxin a decontamination. Toxins 7(4):1151–1162. https://doi.org/10.3390/toxins7041151

Potter PM, Navratilova J, Rogers KR, Al-Abed SR (2019) Transformation of silver nanoparticle consumer products during simulated usage and disposal. Environ Sci Nano 6(2):592–598

Qing Y, Cheng L, Li R, Liu G, Zhang Y, Tang X, Wang J, Liu H, Qin Y (2018) Potential antibacterial mechanism of silver nanoparticles and the optimization of orthopedic implants by advanced modification technologies. Int J Nanomedicine 13:3311–3327. https://doi.org/10.2147/ijn.S165125

Rasool K, Helal M, Ali A, Ren CE, Gogotsi Y, Mahmoud KA (2016) Antibacterial activity of Ti$_3$C$_2$Tx MXene. ACS Nano 10(3):3674–3684. https://doi.org/10.1021/acsnano.6b00181

Riaz M, Sharafat U, Zahid N, Ismail M, Park J, Ahmad B, Rashid N, Fahim M, Imran M, Tabassum A (2022) Synthesis of biogenic silver nanocatalyst and their antibacterial and organic pollutants reduction ability. ACS Omega 7(17):14723–14734. https://doi.org/10.1021/acsomega.1c07365

Ribeiro AI, Dias AM, Zille A (2022) Synergistic effects between metal nanoparticles and commercial antimicrobial agents: a review. ACS Appl Nano Mater 5(3):3030–3064. https://doi.org/10.1021/acsanm.1c03891

Rodríguez-Serrano C, Guzmán-Moreno J, Ángeles-Chávez C, Rodríguez-González V, Ortega-Sigala JJ, Ramírez-Santoyo RM, Vidales-Rodríguez LE (2020) Biosynthesis of silver nanoparticles by Fusarium scirpi and its potential as antimicrobial agent against uropathogenic Escherichia coli biofilms. PLoS ONE 15(3):e0230275. https://doi.org/10.1371/journal.pone.0230275

Saravana Kumar P, Balachandran C, Duraipandiyan V, Ramasamy D, Ignacimuthu S, Al-Dhabi NA (2015) Extracellular biosynthesis of silver nanoparticle using Streptomyces spp. 09 PBT 005 and its antibacterial and cytotoxic properties. Appl Nanosci 5(2):169–180. https://doi.org/10.1007/s13204-014-0304-7

Shah T, Latif S, Saeed F, Ali I, Ullah S, Abdullah Alsahli A, Jan S, Ahmad P (2021) Seed priming with titanium dioxide nanoparticles enhances seed vigor, leaf water status, and antioxidant enzyme activities in maize (Zea mays L.) under salinity stress. J King Saud Univ Sci 33(1):101207. https://doi.org/10.1016/j.jksus.2020.10.004

Shao W, Liu X, Min H, Dong G, Feng Q, Zuo S (2015) Preparation, characterization, and antibacterial activity of silver nanoparticle-decorated graphene oxide nanocomposite. ACS Appl Mater Interfaces 7(12):6966–6973. https://doi.org/10.1021/acsami.5b00937

Sheikh BA, Bhat BA, Mir MA (2022) Antimicrobial resistance: new insights and therapeutic implications. Appl Microbiol Biotechnol 106(19):6427–6440. https://doi.org/10.1007/s00253-022-12175-8

Shu M, He F, Li Z, Zhu X, Ma Y, Zhou Z, Yang Z, Gao F, Zeng M (2020) Biosynthesis and antibacterial activity of silver nanoparticles using yeast extract as reducing and capping agents. Nanoscale Res Lett 15(1):14. https://doi.org/10.1186/s11671-019-3244-z

Shukla R, Nune SK, Chanda N, Katti K, Mekapothula S, Kulkarni RR, Welshons WV, Kannan R, Katti KV (2008) Soybeans as a phytochemical reservoir for the production and stabilization of biocompatible gold nanoparticles. Small 4(9):1425–1436. https://doi.org/10.1002/smll.200800525

Soltys L, Olkhovyy O, Tatarchuk T, Naushad M (2021) Green synthesis of metal and metal oxide nanoparticles: principles of green chemistry and raw materials. Magnetochemistry 7(11):145. https://doi.org/10.3390/magnetochemistry7110145

Su H-L, Chou C-C, Hung D-J, Lin S-H, Pao IC, Lin J-H, Huang F-L, Dong R-X, Lin J-J (2009) The disruption of bacterial membrane integrity through ROS generation induced by nanohybrids of

silver and clay. Biomaterials 30(30):5979–5987. https://doi.org/10.1016/j.biomaterials.2009.07.030

Sundaria N, Singh M, Upreti P, Chauhan RP, Jaiswal JP, Kumar A (2019) Seed priming with iron oxide nanoparticles triggers iron acquisition and biofortification in wheat (Triticum aestivum L.) grains. J Plant Growth Regul 38(1):122–131. https://doi.org/10.1007/s00344-018-9818-7

Tao Z, Yuan H, Liu M, Liu Q, Zhang S, Liu H, Jiang Y, Huang D, Wang T (2023) Yeast extract: characteristics, production, applications and future perspectives. J Microbiol Biotechnol 33(2):151–166. https://doi.org/10.4014/jmb.2207.07057

Taran N, Storozhenko V, Svietlova N, Batsmanova L, Shvartau V, Kovalenko M (2017) Effect of zinc and copper nanoparticles on drought resistance of wheat seedlings. Nanoscale Res Lett 12(1):60. https://doi.org/10.1186/s11671-017-1839-9

Tekin V, Kozgus Guldu O, Dervis E, Yurt Kilcar A, Uygur E, Biber Muftuler FZ (2019) Green synthesis of silver nanoparticles by using eugenol and evaluation of antimicrobial potential. Appl Organomet Chem 33(7):e4969. https://doi.org/10.1002/aoc.4969

Thanh NTK, Maclean N, Mahiddine S (2014) Mechanisms of nucleation and growth of nanoparticles in solution. Chem Rev 114(15):7610–7630. https://doi.org/10.1021/cr400544s

Tomé D (2021) Yeast extracts: nutritional and flavoring food ingredients. ACS Food Sci Technol 1(4):487–494. https://doi.org/10.1021/acsfoodscitech.0c00131

Torky HA, Khaliel SA-E, Sedeek EK, Tawfik RG, Bkheet AAE, Ebied SK, Hs A, Zahran SI, Emara HA-E, Nofal AM, Elghazaly EM (2022) Silver nanoparticle effect on Salmonella enterica isolated from Northern West Egypt food, poultry, and calves. Appl Microbiol Biotechnol 106(17):5701–5713. https://doi.org/10.1007/s00253-022-12102-x

Varjovi MB, Zakaria RA, Rostamnia S, Gholipour B (2023) Biosynthesized Ag nanoparticles on urea-based periodic mesoporous organosilica enhance galegine content in Galega. Appl Microbiol Biotechnol 107(5):1589–1608. https://doi.org/10.1007/s00253-023-12414-6

Venzhik Y, Deryabin A, Popov V, Dykman L, Moshkov I (2022) Priming with gold nanoparticles leads to changes in the photosynthetic apparatus and improves the cold tolerance of wheat. Plant Physiol Biochem 190:145–155. https://doi.org/10.1016/j.plaphy.2022.09.006

Vidyasagar PRR, Singh SK, Singh M (2023) Green synthesis of silver nanoparticles: methods, biological applications, delivery and toxicity. Mater Adv 4(8):1831–1849. https://doi.org/10.1039/D2MA01105K

Yang T, Ma J, Zhen SJ, Huang CZ (2016) Electrostatic assemblies of well-dispersed AgNPs on the surface of electrospun nanofibers as highly active SERS substrates for wide-range pH sensing. ACS Appl Mater Interfaces 8(23):14802–14811. https://doi.org/10.1021/acsami.6b03720

Zaman Y, Ishaque MZ, Ajmal S, Shahzad M, Siddique AB, Hameed MU, Kanwal K, Ramalingam RJ, Selvaraj M, Yasin G (2023) Tamed synthesis of AgNPs for photodegradation and anti-bacterial activity: Effect of size and morphology. Inorg Chem Comm 150:110523. https://doi.org/10.1016/j.inoche.2023.110523

Zheng Y, Wei M, Wu H, Li F, Ling D (2022) Antibacterial Metal Nanoclusters. J Nanobiotechnol 20(1):328. https://doi.org/10.1186/s12951-022-01538-y